Bis(2-diphenylphosphinoxynaphthalen-1-yl)methane: transition metal chemistry, Suzuki cross-coupling reactions and homogeneous hydrogenation of olefins

Benudhar Punji,[a] Joel T. Mague[b] and Maravanji S. Balakrishna*[a]

Received 25th July 2005, Accepted 31st October 2005
First published as an Advance Article on the web 23rd November 2005
DOI: 10.1039/b510589g

Transition metal complexes of bis(2-diphenylphosphinoxynaphthalen-1-yl)methane (**1**) are described. Bis(phosphinite) **1** reacts with Group 6 metal carbonyls, $[Rh(CO)_2Cl]_2$, anhydrous $NiCl_2$, $[Pd(C_3H_5)Cl]_2/AgBF_4$ and $Pt(COD)I_2$ to give the corresponding 10-membered chelate complexes **2**, **3** and **5–8**. Reaction of **1** with $[Rh(COD)Cl]_2$ in the presence of $AgBF_4$ affords a cationic complex, $[Rh(COD)\{Ph_2P(\text{–}OC_{10}H_6)(\mu\text{-}CH_2)(C_{10}H_6O\text{–})PPh_2\text{-}\kappa P,\kappa P\}]BF_4$ (**4**). Treatment of **1** with $AuCl(SMe_2)$ gives mononuclear chelate complex, $[(AuCl)\{Ph_2P(\text{–}OC_{10}H_6)(\mu\text{-}CH_2)(C_{10}H_6O\text{–})PPh_2\text{-}\kappa P,\kappa P\}]$ (**9**) as well as a binuclear complex, $[Au(Cl)\{\mu\text{-}Ph_2P(\text{–}OC_{10}H_6)(\mu\text{-}CH_2)(C_{10}H_6O\text{–})PPh_2\text{-}\kappa P,\kappa P\}AuCl]$ (**10**) with ligand **1** exhibiting both chelating and bridged bidentate modes of coordination respectively. The molecular structures of **2**, **6**, **7**, **9** and **10** are determined by X-ray studies. The mixture of $Pd(OAc)_2$ and **1** effectively catalyzes Suzuki cross-coupling reactions of a range of aryl halides with aryl boronic acid in MeOH at room temperature or at 60 °C, giving generally high yields even under low catalytic loads. The cationic rhodium(I) complex, $[Rh(COD)\{Ph_2P(\text{–}OC_{10}H_6)(\mu\text{-}CH_2)(C_{10}H_6O\text{–})PPh_2\text{-}\kappa P,\kappa P\}]BF_4$ (**4**) catalyzes the hydrogenation of styrenes to afford the corresponding alkyl benzenes in THF at room temperature or at 70 °C with excellent turnover frequencies.

Introduction

Synthesis of novel bisphosphine ligand systems to stabilize platinum metal chelates is considered to be a most challenging task in view of their potential usefulness as homogeneous catalysts for a variety of organic transformations.[1] The ligating properties of these ligands depend to a large extent on the nature of the spacer and also on the phosphorus substituents. In ligands such as binap,[2] restricted rotation makes them excellent ligands for asymmetric synthesis. On the other hand, if the bulky groups can rotate freely about a pivoting group, ring strain can be induced that enhances the rate of dissociation of one of the metal-phosphorus bonds so that it can perform as a better catalyst. In contrast, in such cases, the increase in bite angle will enhance the steric congestion around the metal centre, which favours the less sterically demanding transition state that can lead to selectivity in catalysis.[3] In view of this, recently we have synthesized and reported transition metal complexes of bis(2-diphenylphosphinoxynaphthalen-1-yl)methane (**1**).[4] As a continuation of our work[5] in designing new phosphorus based ligands for exploring their organometallic chemistry and catalytic utility in organic synthesis, herein we report more transition metal complexes of the large-bite bis(phosphinite) **1**. As will be seen, we also show that $Pd(OAc)_2$/**1** exhibits significant catalytic activity in Suzuki cross-coupling reactions and the cationic rhodium complex in catalytic hydrogenation of styrenes. X-Ray structures of molybdenum(0), nickel(II), palladium(II) and gold(I) complexes of **1** are also described.

Results and discussion

Our main objective initially was to explore the coordination behavior of the large-bite bis(phosphinite) ligand (**1**) and to explore its catalytic applications. Previously, we have described the synthesis, derivatization and ruthenium(II), palladium(II) and platinum(II) complexes of **1**.[4] In the present study, more chelate complexes are described. The reaction of **1** with $[Mo(CO)_6]$ or $[W(CO)_4(piperazine)_2]$ in toluene affords the tetracarbonyl derivatives, $[M(CO)_4\{Ph_2P(\text{–}OC_{10}H_6)(\mu\text{-}CH_2)(C_{10}H_6O\text{–})PPh_2\text{-}\kappa P,\kappa P\}]$ in good yield. The IR spectra of complexes **2** and **3** exhibit strong absorptions in the range 1872–2035 cm^{-1} characteristic of phosphine donors bound to a *cis*-$M(CO)_4$ moiety.[5b,6] The ^{31}P NMR spectra of complexes **2** and **3** show single resonances at 144.1 and 121.6 ppm respectively. The coordination shifts for **2** and **3** are 31.9 and 9.4 ppm respectively. The tungsten complex shows $^1J_{WP}$ coupling of 285 Hz. The reaction of two equivalents of **1** with $[Rh(COD)Cl]_2$ in the presence of $AgBF_4$ in a mixture of methanol–dichloromethane affords a cationic chelate complex, $[Rh(COD)\{Ph_2P(\text{–}OC_{10}H_6)(\mu\text{-}CH_2)(C_{10}H_6O\text{–})PPh_2\text{-}\kappa P,\kappa P\}]BF_4$ (**4**) as shown in Scheme 1. The ^{31}P NMR spectrum of **4** shows a doublet centered at 120.9 ppm with a $^1J_{RhP}$ coupling of 171 Hz. The ESI mass spectrum of **4** shows m/z at 879 (100%) corresponding to the cation. The ^1H NMR spectrum of **4** shows a singlet at 4.81 ppm for the bridging methylene group and the resonances due to COD appear as multiplets in the region 2.32–2.72 and 6.02–7.25 ppm. The reaction of **1** with $[Rh(CO)_2Cl]_2$ in a 2 : 1 ratio gives the

---

[a] *Department of Chemistry, Indian Institute of Technology Bombay, Powai, Mumbai, 400 076, India. E-mail: krishna@chem.iitb.ac.in; Fax: +91 22 2576 7152/2572 3480; Tel: +91 22 2576 7181*
[b] *Department of Chemistry, Tulane University, New Orleans, Lousiana, 70118, USA*

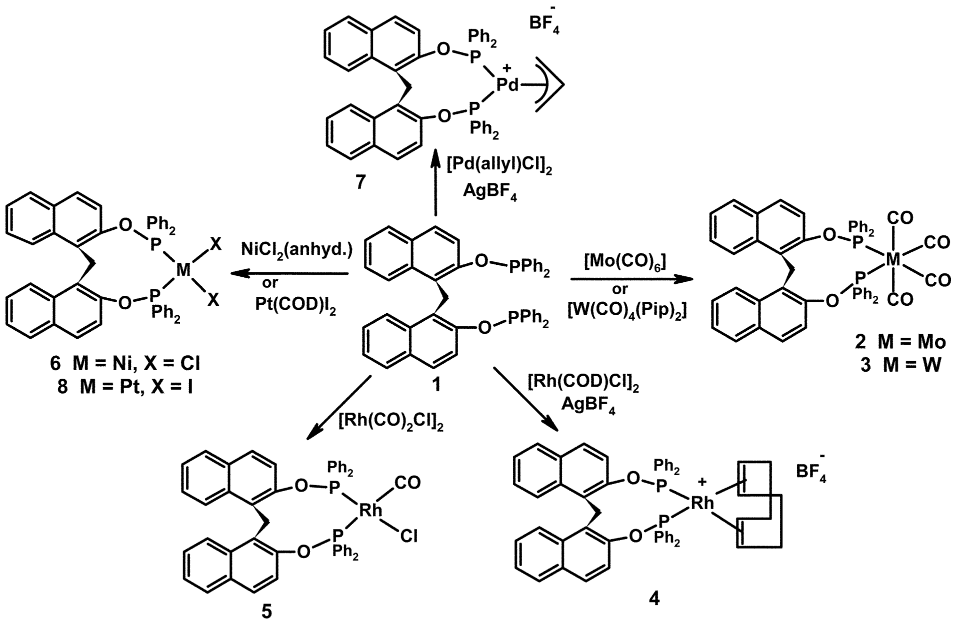

Scheme 1

expected mononuclear complex, $[Rh(Cl)(CO)\{Ph_2P(–OC_{10}H_6)(\mu\text{-}CH_2)(C_{10}H_6O–)PPh_2\text{-}\kappa P,\kappa P\}]$ (**5**), in quantitative yield. The IR spectrum of **5** shows a strong CO absorption at 2037 cm^{-1}, which clearly indicates the *trans* disposition of CO ligand to one of the phosphorus atoms rather than to chlorine.[7] The ^{31}P NMR spectrum of **5** shows two doublet of doublets centered at 125.5 and 123.9 ppm due to the presence of two magnetically non-equivalent phosphorus centers. The corresponding $^1J_{RhP}$ couplings are 187 and 154 Hz respectively. The $^2J_{PP}$ coupling is 38 Hz. The reaction of anhydrous $NiCl_2$ with ligand **1** in THF at room temperature gives a dark red colored square planar complex, $[NiCl_2\{Ph_2P(–OC_{10}H_6)(\mu\text{-}CH_2)(C_{10}H_6O–)PPh_2\text{-}\kappa P,\kappa P\}]$ (**6**) in 52% yield. The ^{31}P NMR spectrum shows a broad singlet at 115.5 ppm. The reaction of **1** with the allyl-palladium dimer, $[Pd(\eta^3\text{-}C_3H_5)Cl]_2$ in a 2 : 1 ratio in the presence of two equivalents of $AgBF_4$ affords a chelate complex, $[Pd(C_3H_5)\{Ph_2P(–OC_{10}H_6)(\mu\text{-}CH_2)(C_{10}H_6O–)PPh_2\text{-}\kappa P,\kappa P\}]BF_4$ (**7**) in 76% yield. The ^{31}P NMR spectrum of **7** shows a single resonance at 121.8 ppm. The ^1H NMR spectrum and the microanalysis of complex **7** agree well with the proposed molecular composition. The molecular structure of **7** is also confirmed by a single crystal X-ray analysis. The reaction of **1** with $[Pt(COD)I_2]$ in dichloromethane in a 1 : 1 ratio gives *cis*-$[PtI_2\{Ph_2P(–OC_{10}H_6)(\mu\text{-}CH_2)(C_{10}H_6O–)PPh_2\text{-}\kappa P,\kappa P\}]$ (**8**) in 88% yield. The ^{31}P NMR spectrum of **8** exhibits a singlet at 87.3 ppm with a large $^1J_{PtP}$ coupling of 3896 Hz, which is consistent with the proposed *cis*-geometry.[4,5b] The reaction of **1** with $[AuCl(SMe_2)]$ in a 1 : 1 ratio in dichloromethane gives a chelate complex, $[AuCl\{Ph_2P(–OC_{10}H_6)(\mu\text{-}CH_2)(C_{10}H_6O–)PPh_2\text{-}\kappa P,\kappa P\}]$ (**9**) whereas a similar reaction with two equivalents of $[AuCl(SMe_2)]$ affords a dinuclear complex, $[AuCl\{\mu\text{-}Ph_2P(–OC_{10}H_6)(\mu\text{-}CH_2)(C_{10}H_6O–)PPh_2\text{-}\kappa P,\kappa P\}AuCl]$ (**10**) with ligand **1** exhibiting the bridged bidentate mode of coordination (Scheme 2). The ^{31}P NMR spectra of complexes **9** and **10** show single resonances at 136.1 and 111.7 ppm, respectively. Further evidence for the molecular composition of complexes **9** and **10** comes from the elemental analysis, mass spectrometry and the single-crystal X-ray diffraction studies.

The crystal and molecular structures of 2, 6, 7, 9 and 10

Perspective views of the molecular structures of compounds **2**, **6**, **7**, **9** and **10** with the atom numbering schemes are shown in Fig. 1–5 respectively. Crystal data and the details of the structure determination are given in Table 1, while selected bond lengths and bond angles appear below the corresponding Figures.

In the structure of **2**, the molybdenum atom shows distorted octahedral geometry with four terminal carbonyls and ligand **1** chelating in a *cis* fashion with a bite angle of 95.06(3)°. There is no significant difference in the Mo–C bond distances for carbonyl groups having *cis* and *trans* dispositions with respect to the phosphorus centers. The average C–O distance is 1.145(4) Å. In the structure of **6**, the nickel center adopts almost square planar

Scheme 2

Table 1 Crystallographic data for **2**, **6**, **7**, **9** and **10**

	2	**6**	**7**	**9**	**10**
Formula	$C_{49}H_{34}MoO_6P_2\cdot CH_2Cl_2$	$C_{45}H_{34}Cl_2NiO_2P_2\cdot CH_2Cl_2$	$C_{48}H_{39}BF_4O_2P_2Pd\cdot 2CH_2Cl_2$	$C_{45}H_{34}AuClO_2P_2\cdot CH_2Cl_2$	$C_{45}H_{34}Au_2Cl_2O_2P_2$
M	961.57	883.18	1072.79	986.05	1133.49
Crystal system	Triclinic	Monoclinic	Monoclinic	Triclinic	Monoclinic
Space group	$P\bar{1}$ (no. 2)	$P2_1/c$ (no. 14)	$P2_1/n$ (no. 14)	$P\bar{1}$ (no. 2)	$P2_1/n$ (no. 14)
a/Å	10.726(1)	15.008(1)	19.924(2)	12.337(1)	16.935(2)
b/Å	11.460(1)	10.949(1)	10.741(1)	12.453(1)	12.521(2)
c/Å	17.609(1)	26.287(2)	22.488(2)	12.806(1)	20.620(3)
α/°	77.918(1)	90	90	84.941(1)	90
β/°	83.014(1)	105.429(1)	108.071(1)	88.464(1)	98.936(2)
γ/°	88.284(1)	90	90	78.992(1)	90
V/Å^3	2100.8(2)	4163.8(5)	4575.1(7)	1923.6(3)	4319.3(11)
Z	2	4	4	2	4
D_c/g cm^{-3}	1.520	1.409	1.558	1.699	1.743
μ/mm^{-1}	0.568	0.838	0.767	4.156	7.018
T/K	100	100	100	100	100
$\theta_{\text{min, max}}$/°	1.8, 28.3	1.4, 28.3	1.6, 28.3	1.6, 27.5	1.5, 24.7
$R_1{}^a$	0.0496	0.0410	0.0548	0.0346	0.0576
$wR_2{}^b$	0.1120	0.1061	0.1483	0.0920	0.1247

^{a} $R_1 = \sum F_o - F_c/\sum F_o$. ^{b} $wR_2 = \{\sum w[(F_o{}^2 - F_c{}^2)^2]/\sum[w(F_o{}^2)^2]\}^{1/2}$.

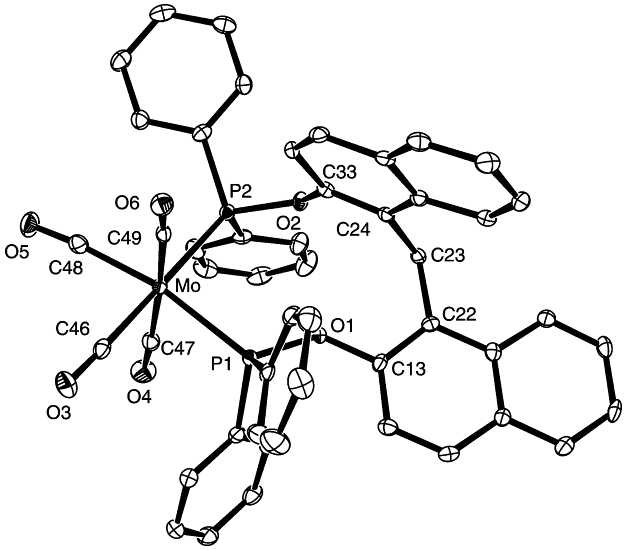

Fig. 1 Molecular structure of **2**·CH$_2$Cl$_2$. For clarity, solvent and all hydrogen atoms have been omitted. Thermal ellipsoids are drawn at the 50% probability level. Selected bond distances (Å) and angles (°): Mo–P(1) 2.479(1), Mo–P(2) 2.520(1), P(1)–O(1) 1.640(2), P(2)–O(2) 1.644(2), Mo–C(46) 2.008(3), Mo–C(48) 2.000(3), Mo–C(47) 2.063(3), Mo–C(49) 2.031(3), O(3)–C(46), O(5)–C(48), O(6)–C(49) 1.145(4), O(4)–C(47) 1.135(4); P(1)–Mo–P(2) 95.06(3), P(1)–Mo–C(46) 85.44(10), P(1)–Mo–C(48) 169.39(9), C(46)–Mo–C(48) 84.56(13), C(22)–C(23)–C(24) 114.2(3).

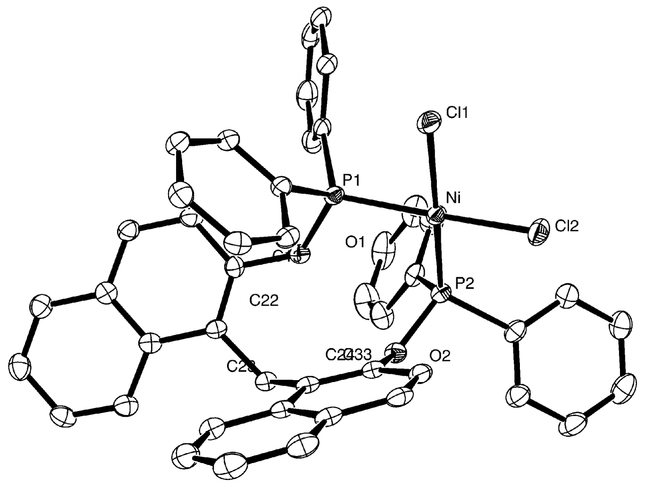

Fig. 2 Molecular structure of **6**·CH$_2$Cl$_2$. For clarity, solvent and all hydrogen atoms have been omitted. Thermal ellipsoids are drawn at the 50% probability level. Selected bond distances (Å) and angles (°): Ni–Cl(1) 2.192(1), Ni–Cl(2) 2.177(1), Ni–P(1) 2.166(1), Ni–P(2) 2.169(1), P(1)–O(1) 1.636(1), P(2)–O(2) 1.620(1); Cl(1)–Ni–Cl(2) 91.33(2), Cl(1)–Ni–P(1) 81.38(2), Cl(1)–Ni–P(2) 173.06(2), Cl(2)–Ni–P(1) 169.39(2), P(1)–Ni–P(2) 95.96(2), C(22)–C(23)–C(24) 117.04(17).

Table 2 Bite angles (°) in chelate complexes of **1** (LL)

Compound	Bite angle		Ref.
M(CO)$_4$(LL)	P(1)–Mo–P(2)	95.06(3)	This work
CpRuCl(LL)	P(1)–Ru–P(2)	93.94(7)	4
NiCl$_2$(LL)	P(1)–Ni–P(2)	95.96(2)	This work
[(C$_3$H$_5$)Pd(LL)]BF$_4$	P(1)–Pd–P(2)	98.95(3)	This work
PtCl$_2$(LL)	P(1)–Pt–P(2)	95.37(9)	4
AuCl(LL)	P(1)–Au(1)–P(2)	132.56(4)	This work

geometry and the bis(phosphinite) makes a twisted 10-membered chelate ring with one of the naphthalene rings oriented almost orthogonal to the plane of the ring. Similarly, the palladium center in structure **7** also adopts a distorted square planar geometry, where the bisphosphinite ligand shows chelating mode of coordination with slight difference in Pd–P(1) and Pd–P(2) bond lengths. The P–M–P bite angles for **6** and **7** are 95.96(2) and 98.95(3)°, respectively, which are comparable with those of the ruthenium(II) (93.94(7)°) and platinum(II) (95.37(9)°) analogues[4] (see Table 2). Interestingly, the P–O bond distances in the nickel complex are comparable with those found in ruthenium complex, whereas the bond distances shrink in the palladium complex and further shrinking was observed in platinum complex, which may be due to the size of metal atoms. The average O–C(aromatic) bond

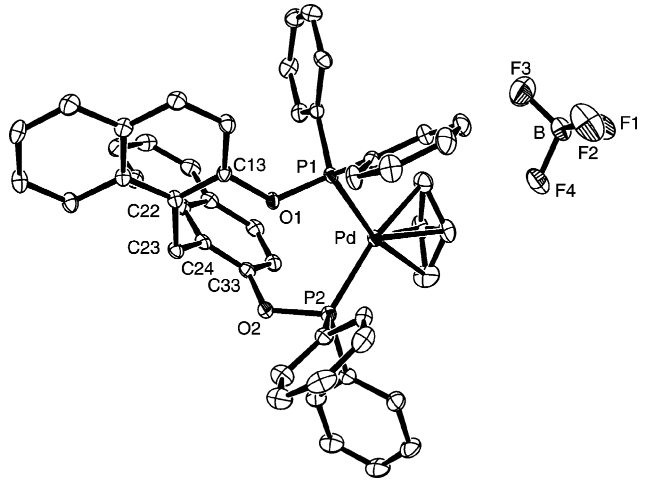

Fig. 3 Molecular structure of $7{\cdot}2CH_2Cl_2$. For clarity solvent and all hydrogen atoms have been omitted. Thermal ellipsoids are drawn at the 50% probability level. Selected bond distances (Å) and angles (°): Pd–P(1) 2.291(1), Pd–P(2) 2.288(1), Pd–C(46) 2.186(6), Pd–C(47) 2.163(8), Pd–C(48) 2.185(4), P(1)–O(1) 1.623(3), P(2)–O(2) 1.628(3); P(1)–Pd–P(2) 98.95(3), P(1)–Pd–C(46) 163.81(12), P(1)–Pd–C(47) 129.23(17), P(1)–Pd–C(48) 96.61(11), C(22)–C(23)–C(24) 114.5(3).

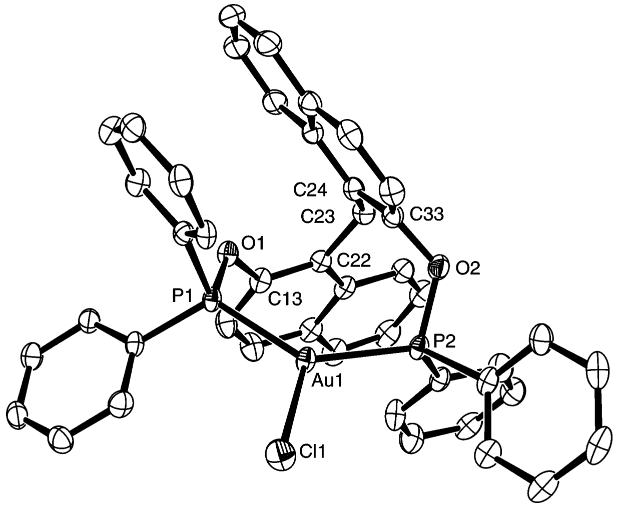

Fig. 4 Molecular structure of $9{\cdot}CH_2Cl_2$. For clarity solvent and all hydrogen atoms have been omitted. Thermal ellipsoids are drawn at the 50% probability level. Selected bond distances (Å) and angles (°): Au(1)–Cl(1) 2.506(1), Au(1)–P(1) 2.293(1), Au(1)–P(2) 2.294(1), P(1)–O(1) 1.639(3), P(2)–O(2) 1.637(3); Cl(1)–Au(1)–P(1) 113.28(4), Cl(1)–Au(1)–P(2) 113.73(4), P(1)–Au(1)–P(2) 132.56(4), C(22)–C(23)–C(24) 122.2(3).

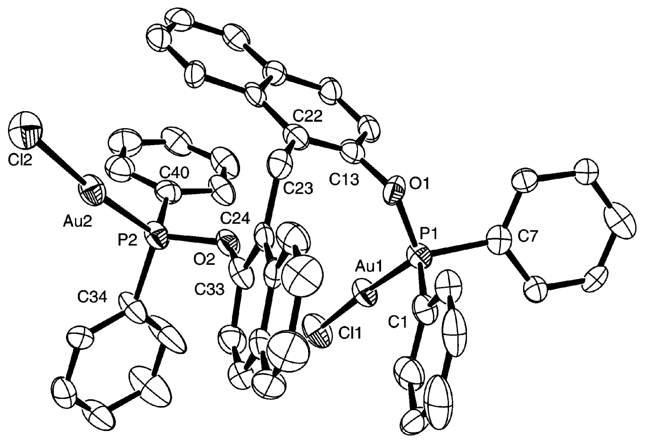

Fig. 5 Molecular structure of **10**. For clarity, all hydrogen atoms have been omitted. Thermal ellipsoids are drawn at the 50% probability level. Selected bond distances (Å) and angles (°): Au(1)–Cl(1) 2.276(3), Au(1)–P(1) 2.210(3), Au(2)–Cl(2) 2.287(3), Au(2)–P(2) 2.211(3), P(1)–O(1) 1.604(7); Cl(1)–Au(1)–P(1) 176.83(13), Cl(2)–Au(2)–P(2) 174.63(11), Au(1)–P(1)–O(1) 116.2(3), C(22)–C(23)–C(24) 119.0(9).

distance is 1.40 Å. The Ni–P distances (2.166(1) Å) are the shortest in the series while the Ru–P bond distances are the longest (2.254(2) Å), which indicate the better π-donor capability of nickel center as compared to the ruthenium center. In the structures of **9** and **10**, the gold centers adopt trigonal planar and linear geometries respectively. The angles around the gold center in **9** are 360° with a P–Au–P angle of 132.56(4)°. Because of this large bite angle the angle at the bridgehead methylene carbon is 122.2(3)°, which is approximately 6–8° greater than those found in the other chelate complexes of **1**. In complex **10**, the two Au–Cl units adopt anti positions that situate the metal atoms at a longer distance (6.685 Å) from each other, preventing the formation of an aurophilic contact. The geometry around the metals is almost linear, with P–Au–Cl angles of 176.83(13) and 174.63(11)°. The dinaphthol backbone is almost perpendicular with a torsion angle of 106.19°.

A close look at the way the molecules are packed in the crystal shows the presence of intermolecular CH–Cl contacts (see Fig. 6). Although, the two Au–Cl units of adjacent molecules are situated in an antiparallel manner, there is no intermolecular Au–Cl contact (7.27 Å).

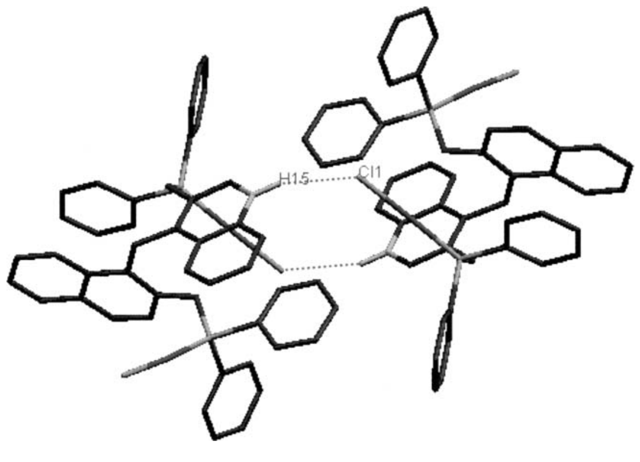

Fig. 6 Intermolecular interactions in **10** [Cl(1) · · · H(15) 2.905 Å (most H atoms are omitted for clarity)].

Suzuki cross-coupling reactions

A mixture of $Pd(OAc)_2$ and **1** effectively catalyzes the Suzuki cross-coupling reactions of a variety of aryl halides and aryl boronic acids affording the desired biaryls in remarkably high yields (Table 3). For example, in a solution of $Pd(OAc)_2/\mathbf{1}$ (0.5 mol%) in MeOH containing K_2CO_3 (2 equiv.), 4-bromobenzaldehyde couples with phenyl boronic acid to give quantitative yield of 4-formylbiphenyl at room temperature after 1 h (entry 1). It is notable that the use of deactivated, electron rich aryl bromides

Table 3 Suzuki cross-coupling of aryl halides with boronic acids catalyzed by $Pd(OAc)_2$/**1**

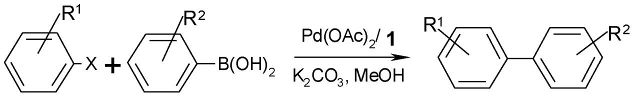

Entry	Aryl halide	Boronic acid	Product	Conditions[a]	Conversion[b] (%)
1	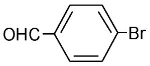	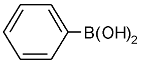	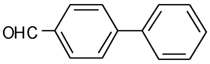	0.5 mol%, R.T., 1 h	100
2	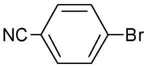	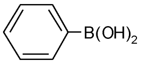	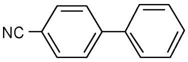	0.5 mol%, R.T., 1 h	>99
3	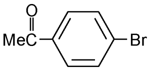	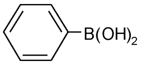	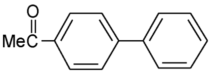	0.5 mol%, R.T., 1 h	97
4	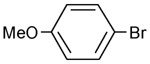	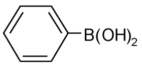	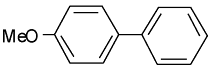	0.5 mol%, R.T., 1 h	79 (90)[c]
5	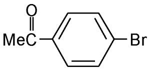	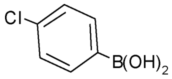	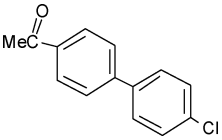	0.5 mol%, R.T., 1 h	98
6	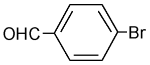	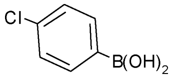	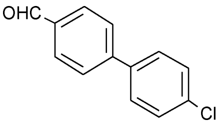	0.5 mol%, R.T., 1 h	87
7	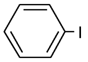	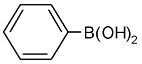	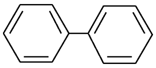	0.5 mol%, R.T., 1 h	80 (99)[c]
8	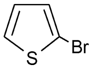	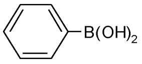	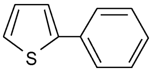	1 mol%, 60 °C, 2 h	92
9	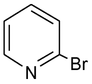	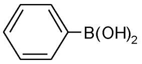	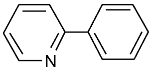	1 mol%, 60 °C, 2 h	57
10	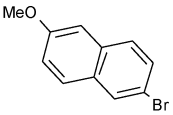	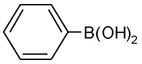	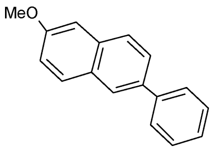	1 mol%, 60 °C, 2 h	83
11	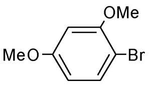	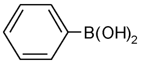	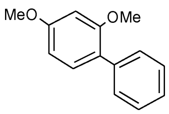	1 mol%, 60 °C, 1 h	34

[a] Aryl halide (0.5 mmol), aryl boronic acid (0.75 mmol), K_2CO_3 (1 mmol), MeOH (5 mL). [b] Conversion to coupled product determined by GC, based on aryl halides; average of two runs. [c] At 60 °C, 1 h.

(*e.g.* entry 4) as well as activated, electron poor ones (*e.g.* entry 1) also resulted in high yields. In general, this coupling can be satisfactorily carried out at room temperature. When there is a need to improve the yield, it can be carried out at elevated (60 °C) temperature (see entries 4 and 7). We also studied the coupling of aryl bromides with some substituted boronic acid (entries 5 and 6), which gave near-quantitative yields at room temperature. The coupling of some heterocycles and sterically bulky aryl bromides with boronic acids tend to give moderate yields (entries 8 and 10). For example, the coupling of 2-bromo-6-methoxynaphthalene with phenyl boronic acid in the presence of 1 mol% of catalyst at 60 °C for 2 h, gives 2-phenyl-6-methoxynaphthalene in 83% yield (entry 10) whereas 2,4-dimethoxybromobenzene resists coupling with phenyl boronic acid (entry 11).

The high efficiency of $Pd(OAc)_2$/**1** at room temperature or 60 °C makes this a valuable catalyst for thermally sensitive substrates. To our knowledge, there have been only a few reports on efficient Suzuki cross-coupling reactions of aryl bromides at room temperature, most of which are with electron rich phosphine systems: *e.g.* use of the $Pd(OAc)_2$/aminophosphine and $Pd(OAc)_2/(o\text{-biphenyl})P(^tBu)_2$ by Buchwald *et al.*[8] and $Pd_2(dba)_3/P(^tBu)_3$ by Fu *et al.*[9] However, reports on Pd/phosphinite systems are rarely seen in the literature.

The activity of $Pd(OAc)_2$/**1** is found to be superior to that of $PdCl_2(dppf)$, which catalyzes the reaction between 4-bromoacetophenone and phenyl boronic acid in toluene at 70 °C in 94% yield.[10] In comparison with the other phosphinite based palladium catalysts, the catalytic activity of $Pd(OAc)_2$/**1** is similar to that found with the palladium bis(phosphinite), PCP-pincer system, whose reactions were carried out in toluene at 130 °C,[11] and an orthopalladated phosphinite complex carried out at 110 °C.[12]

It is important to achieve good yields using minimum amounts of catalysts. We therefore examined the effect of catalyst loading on a convenient coupling between 4-bromobenzaldehyde and phenyl boronic acid (Table 4). High yields are maintained from normal catalyst loads down to a level of 0.0312 mol%. A moderate yield (61 and >33%) is achieved even at catalyst loading as low as 0.0156 and 0.0078 mol% with a TON of 3905 and 4225, respectively. These are indications of an effective catalytic system that merits more downstream explorations.

Hydrogenation reactions

More interestingly, we found that rhodium complex **4** can be employed in the catalytic hydrogenation of styrene and its derivatives such as 4-methylstyrene and α-methylstyrene (Table 5). For all three substrates, the hydrogenation reactions were performed at 25 °C as well as at 70 °C under 100 psi of H_2 pressure in the presence of triethylamine as a base and THF as solvent. The catalyst was found to be considerably more efficient in terms of conversion under mild conditions than the ruthenium(II) catalyst, $[RuCl_2(p\text{-cymene})(PPh_2Py)]$, employed by Moldes, for the hydrogenation of styrenes.[13] As shown in Table 5, the catalyst exhibits a good conversion of styrene and 4-methylstyrene to yield ethyl benzene and 4-methyl ethyl benzene, respectively. The reaction rate is marginally temperature dependent. Thus, at 25 °C, the styrene hydrogenation shows a TOF value of 333.3 h^{-1} and on increasing the temperature to 70 °C, TOF increases to only 388 h^{-1}. Interestingly, 4-methylstyrene is hydrogenated with TOF values of 500 and 1000 h^{-1} at 25 and 70 °C, respectively. However, the hydrogenation of α-methylstyrene at 25 °C is slow with a TOF value of only 89.9 h^{-1} with 54% conversion after 6 h. When the temperature

Table 4 Influence of low catalyst loading on the coupling reaction

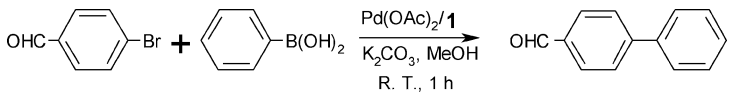

Entry	Amount of catalyst $Pd(OAc)_2$/**1** (mol%)	Conversion (%)	TON[a]
1	0.5	100	200
2	0.25	99	396
3	0.125	99	792
4	0.0625	99	1584
5	0.0312	91	2912
6	0.0156	61	3905
7	0.0078	33	4225

[a] In units of mol product (mol Pd)$^{-1}$.

Table 5 Catalytic olefin hydrogenation reactions[a]

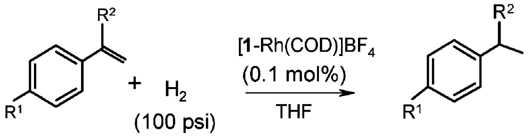

Substrate	T/°C	t/h	Conversion (%)	TOF[b]/h^{-1}
$R^1 = R^2 = H$	25	3	100	333.3
$R^1 = R^2 = H$	70	2.5	97	388
$R^1 = Me, R^2 = H$	25	2	100	500
$R^1 = Me, R^2 = H$	70	1	100	1000
$R^1 = H, R^2 = Me$	25	6	54	89.9
$R^1 = H, R^2 = Me$	70	2	97	485
$R^1 = H, R^2 = Me$ (no catalyst)	70	6	6	9.9

[a] *Conditions*: The molar ratio of substrate to base (Et_3N) to catalyst was 1000 : 50 : 1; $p(H_2)$ = 100 psi. Solvent THF (20 mL). [b] TOF expressed as moles of substrate converted to product per mole of catalyst per hour. Products were ascertained by GC analysis (based on conversion of styrenes).

was increased to 70 °C, it showed good conversion with TOF value of 485 h^{-1}. One run was performed on α-methylstyrene at 70 °C without catalyst which showed only 6% conversion after 6 h. The homogeneous nature of the catalysis was checked by the classical mercury test.[14] Addition of a drop of mercury to the reaction mixtures did not affect the yields of the hydrogenations thus showing them to be truly homogeneous systems.

From the reaction profile, we can deduce that, 4-methylstyrene is hydrogenated faster than styrene or α-methylstyrene. Probably, the *para* substituents on the benzene ring enhanced the reaction rate whereas the substituents on olefinic carbons controlled the reaction rate due to the steric attributes. It would be interesting to examine the regioselectivity in the hydrogenations of a less substituted olefin site in the presence of highly substituted olefin centers. The work in this direction is underway.

Summary

In conclusion, the bis(phosphinite) **1** is a versatile and electron-rich bidentate ligand which forms complexes with most of the transition metals. With gold(I) derivatives it forms both mononuclear and binuclear complexes with the ligand exhibiting chelating and bridged bidentate modes of coordination. The use of $Pd(OAc)_2$/**1** demonstrated that we can achieve very high yields under mild conditions in Suzuki cross-coupling for both activated and inactivated aryl bromides. The cationic rhodium(I) complex (**4**) shows excellent catalytic activity in the hydrogenation of styrenes in as low as 0.1 mol% concentrations. The ease of synthesis, moderate stability towards moisture and flexible ligand skeleton and excellent turnover numbers in the hydrogenation reactions are promising features of this large-bite ligand system. It has also encouraged us to examine other catalytic systems beyond the hydrogenation and Suzuki coupling reactions. Further utility of this ligand in several other hydrogenation processes and C–C coupling reactions of stubborn aryl chlorides is under active investigation in our laboratory.

Experimental

All experimental manipulations were carried out under an atmosphere of dry nitrogen or argon using Schlenk techniques. Solvents were dried and distilled prior to use by conventional methods. Bis(phosphinite) **1**,[4] $[W(CO)_4(NHC_5H_{10})_2]$,[15] $[Rh(COD)Cl]_2$,[16] $[Rh(CO)_2Cl]_2$,[17] $[(\eta^3\text{-}C_3H_5)PdCl]_2$,[18] $[Pt(COD)I_2]$,[19] $[AuCl(SMe_2)]$,[20] were prepared according to the published procedures. The ^1H and $^{31}P\{^1H\}$ NMR (δ in ppm) spectra were obtained on a Varian VXR 300 or VRX 400 spectrometer operating at frequencies of 300 or 400 and 121 or 162 MHz, respectively. The spectra were recorded in $CDCl_3$ (or DMSO-d_6) solutions with $CDCl_3$ (or DMSO-d_6) as an internal lock; TMS and 85% H_3PO_4 were used as internal and external standards for ^1H and $^{31}P\{^1H\}$ NMR, respectively. Positive shifts lie downfield of the standard in all of the cases. Infrared spectra were recorded on a Nicolet Impact 400 FTIR instrument as a KBr disk or Nujol mull. Microanalyses were carried out on a Carlo Erba Model 1106 elemental analyzer. Q-Tof Micromass experiments were carried out using Waters Q-Tof micro(YA-105). Melting points of all compounds were determined on Veego melting point apparatus and were uncorrected. GC analyses were performed on a Perkin Elmer Clarus 500 GC fitted with packed column.

Synthesis of $[Mo(CO)_4\{\eta^2\text{-}Ph_2P(\text{–}OC_{10}H_6)(\mu\text{-}CH_2)(C_{10}H_6O\text{–})PPh_2\text{-}\kappa P,\kappa P\}]$ (2)

A mixture of the ligand **1** (0.106 g, 0.16 mmol) and $Mo(CO)_6$ (0.04 g, 0.15 mmol) in 12 mL of toluene was heated at 90 °C for 10 h to give a clear yellowish solution. The solvent was removed under reduced pressure to give a sticky residue. The residue was dissolved in CH_2Cl_2 (2 mL), layered with petroleum ether (1 mL; bp 60–80 °C) and was cooled to −25 °C to afford colourless crystals of **2**. Yield: 49% (0.064 g). Mp 138 °C (decomp.). Anal. Calc. for $C_{49}H_{34}MoO_6P_2$: C, 67.13; H, 3.91%. Found: C, 66.93; H, 3.84%. FT IR (KBr disk) cm^{-1}: ν_{CH}: 3058 s; ν_{CO}: 2034 s, 1922 vs, 1912 vs, 1892 vs. ^1H NMR (400 MHz, $CDCl_3$): δ 8.13 (d, 2H, Ar) 7.69 (d, 2H, Ar), 7.49 (br s, 2H, Ar), 7.17–7.35 (m, 4H, Ar, 20H, $OPPh_2$), 6.79 (d, 2H, Ar), 5.25 (s, 2H, Ar–CH_2–Ar). $^{31}P\{^1H\}$ NMR (161.9 MHz, $CDCl_3$): δ 144.1 (s).

Synthesis of $[W(CO)_4\{\eta^2\text{-}Ph_2P(\text{–}OC_{10}H_6)(\mu\text{-}CH_2)(C_{10}H_6O\text{–})PPh_2\text{-}\kappa P,\kappa P\}]$ (3)

A mixture of the ligand **1** (0.075 g, 0.112 mmol) and $[W(CO)_4(NHC_5H_{10})_2]$ (0.05 g, 0.107 mmol) in 12 mL of toluene was heated at 90 °C for 18 h, which was then allowed to come to room temperature and filtered. The solvent was removed under vacuum to give yellow residue, which was washed with petroleum ether thrice and dried. The residue was dissolved in CH_2Cl_2 (3 mL), and layered with petroleum ether (1 mL), which on cooling to −25 °C gave analytically pure, crystalline product of **3**. Yield: 83% (0.086 g). Mp 168 °C (decomp.). Anal. Calc. for $C_{49}H_{34}WO_6P_2$: C, 61.01; H, 3.55%. Found: C, 60.92; H, 3.45%. FT IR (KBr disk) cm^{-1}: ν_{CH}: 3053 s; ν_{CO}: 2025 s, 1949 vs, 1912 vs, 1873 vs. ^1H NMR (400 MHz, $CDCl_3$): δ 8.23 (d, 2H, Ar), 8.14 (d, 2H, Ar), 7.12 (d, 2H, Ar), 7.62–7.81 (m, 4H, Ar), 7.18–7.57 (m, 20H, $OPPh_2$), 6.78 (d, 2H, Ar), 4.74 (s, 2H, Ar–CH_2–Ar). $^{31}P\{^1H\}$ NMR (161.9 MHz, $CDCl_3$): δ 121.6 (s), $^1J_{WP}$ = 285 Hz.

Synthesis of $[Rh(COD)\{\eta^2\text{-}Ph_2P(\text{–}OC_{10}H_6)(\mu\text{-}CH_2)(C_{10}H_6O\text{–})PPh_2\text{-}\kappa P,\kappa P\}]BF_4$ (4)

$AgBF_4$ (0.021 g, 0.11 mmol) was added to the stirred solution of $[Rh(COD)Cl]_2$ (0.025 g, 0.051 mmol) in 8 mL of methanol. After 30 min, a solution of the ligand **1** (0.074 g, 0.11 mmol) in 6 mL of CH_2Cl_2 was added dropwise and stirred for 4 h. The suspension obtained was filtered to remove AgCl, and the yellowish-orange filtrate was concentrated to 5 mL. Cooling this solution to −25 °C, gave **4** as an analytically pure yellow crystalline solid. Yield: 66% (0.07 g). Mp 174 °C (decomp.). Anal. Calc. for $C_{53}H_{46}BF_4O_2P_2Rh$: C, 65.85; H, 4.79%. Found: C, 65.88; H, 4.63%. ^1H NMR (400 MHz, $CDCl_3$): δ 8.03 (d, 2H, Ar), 7.77 (d, 2H, Ar), 7.75 (br s, 2H, Ar), 7.69 (br s, 2H, Ar), 7.41–7.56 (m, 20H, $OPPh_2$), 7.38 (m, 2H, Ar), 7.29 (m, 2H, Ar), 6.02–7.25 (m, 4H, (COD)), 4.81 (s, 2H, Ar–CH_2–Ar), 2.32–2.72 (m, 8H, (COD)). $^{31}P\{^1H\}$ NMR (161.9 MHz, $CDCl_3$): δ 120.9 (d, $^1J_{RhP}$ = 171 Hz). ESI MS: 879 ($M^+ - BF_4$).

Synthesis of $[Rh(CO)\{\eta^2\text{-}Ph_2P(\text{–}OC_{10}H_6)(\mu\text{-}CH_2)(C_{10}H_6O\text{–})PPh_2\text{-}\kappa P,\kappa P\}Cl]$ (5)

A solution the ligand **1** (0.105 g, 0.158 mmol) in 8 mL of CH_2Cl_2 was added dropwise to a solution of $[Rh(CO)_2Cl]_2$ (0.03 g, 0.077 mmol), also in CH_2Cl_2 (6 mL). The reaction mixture was heated to reflux for 4 h, after which the solution was allowed to come to room temperature. The yellow colored solution was concentrated to 3 mL, layered with diethyl ether (1 mL), and cooled to −25 °C to give **5** as an analytically pure, yellow crystalline solid. Yield: 94% (0.12 g). Mp 136 °C (decomp.). Anal. Calc. for $C_{46}H_{34}ClO_3P_2Rh$: C, 66.16; H, 4.10%. Found: C, 65.96; H, 3.93%. IR (Nujol, ν_{CO}, cm^{-1}): 2037 s. ^1H NMR (400 MHz, $CDCl_3$): δ 8.02 (d, 2H, Ar), 7.75–7.80 (m, 4H, Ar), 7.25–7.72 (m, 6H, Ar and 20H, $OPPh_2$), 4.79 (s, 2H, Ar–CH_2–Ar). $^{31}P\{^1H\}$ NMR (121.4 MHz, $CDCl_3$): δ 125.5 (dd, $^1J_{RhP}$ = 187 Hz), δ 123.9 (dd, $^1J_{RhP}$ = 154 Hz), $^2J_{PP}$ = 38 Hz.

Synthesis of [$NiCl_2\{\eta^2$-$Ph_2P(–OC_{10}H_6)(\mu$-$CH_2)(C_{10}H_6O–)$-PPh_2-κ*P*,κ*P*}] (6)

A suspension of the ligand **1** (0.107 g, 0.16 mmol) and $NiCl_2$ (0.02 g, 0.15 mmol) in 10 mL of THF was stirred at room temperature for 20 h. The unreacted $NiCl_2$ was removed by filtration. The solvent was removed under reduced pressure to afford a sticky residue. The residue was dissolved in CH_2Cl_2 (3 mL), and layered with petroleum ether (1 mL), which on slow evaporation gave red colored crystals of **6** suitable for X-ray analysis. Yield: 52% (0.062 g). Mp 216 °C (decomp.). Anal. Calc. for $C_{45}H_{34}Cl_2O_2P_2Ni$: C, 67.70; H, 4.29%. Found: C, 67.78; H, 4.33%. ^1H NMR (400 MHz, $CDCl_3$): δ 8.22 (d, 2H, Ar), 8.09 (d, 2H, Ar), 7.81 (br s, 2H, Ar), 7.48–7.73 (m, 20H, $OPPh_2$), 7.43 (br s, 2H, Ar), 7.34 (br s, 2H, Ar), 6.84 (br s, 2H, Ar), 4.79 (s, 2H, Ar–CH_2–Ar). $^{31}P\{^1H\}$ NMR (121.4 MHz, $CDCl_3$): δ 115.5 (br s).

Synthesis of [(η^3-C_3H_5)Pd{η^2-$Ph_2P(–OC_{10}H_6)(\mu$-$CH_2)(C_{10}H_6O–)$-PPh_2-κ*P*,κ*P*}]BF_4 (7)

A solution of [(η^3-C_3H_5)PdCl]$_2$ (0.02 g, 0.055 mmol) in 6 mL of CH_2Cl_2 was added dropwise to a stirred solution of the ligand **1** (0.075 g, 0.112 mmol), also in CH_2Cl_2 (8 mL) at room temperature. After 2 h, $AgBF_4$ (0.022 g, 0.112 mmol) was added to the pale yellow solution and stirring was continued for an additional 30 min. The suspension was filtered through a pad of Celite, the solution was concentrated to 3 mL under reduced pressure, and the product precipitated with petroleum ether. The light yellow product was dissolved in 5 mL of CH_2Cl_2, and layered with petroleum ether (1 mL), which on slow evaporation gave **7** as analytically pure, light-yellow crystals. Yield: 76% (0.075 g). Mp 182 °C (decomp.). Anal. Calc. for $C_{48}H_{39}BF_4O_2P_2Pd$: C, 63.84; H, 4.35%. Found: C, 63.73; H, 4.32%. ^1H NMR (400 MHz, $CDCl_3$): δ 8.01 (br s, 2H, Ar), 7.78 (d, 2H, Ar), 7.59 (d, 2H, Ar), 7.34–7.39 (m, 20H, $OPPh_2$), 7.03–7.26 (br, 4H, Ar), 6.96 (d, 2H, Ar), 5.90–5.92 (m, 1H, allyl), 5.05 (d, 4H, allyl), 4.95 (s, 2H, Ar–CH_2–Ar). $^{31}P\{^1H\}$ NMR (161.9 MHz, $CDCl_3$): δ 121.8 (s).

Synthesis of [$PtI_2\{\eta^2$-$Ph_2P\{$-$OC_{10}H_6)(\mu$-$CH_2)(C_{10}H_6O$-$\}$-PPh_2-κ*P*,κ*P*}] (8)

A solution of the ligand **1** (0.05 g, 0.075 mmol) in 8 mL of CH_2Cl_2 was added dropwise to a solution of [Pt(COD)I_2] (0.04 g, 0.072 mmol) also in CH_2Cl_2 (6 mL) at room temperature. The reaction mixture was stirred for 6 h to give a clear yellow solution. The solvent was removed under reduced pressure to afford a yellow residue, which was washed thrice with petroleum ether and dried. The residue was redissolved in CH_2Cl_2 (3 mL), and layered with 1 mL of petroleum ether, which on cooling to −25 °C gave analytically pure, yellow crystalline product of **8.** Yield: 88% (0.071 g). Mp 204 °C (decomp.). Anal. Calc. for $C_{45}H_{34}I_2O_2P_2Pt$: C, 48.36; H, 3.07%. Found: C, 48.33; H, 2.92%. ^1H NMR (400 MHz, DMSO-d_6): δ 8.08 (br s, 2H, Ar), 7.81 (d, 2H, Ar), 7.59–7.62 (m, 4H, Ar), 7.41–7.51 (m, 20H, $OPPh_2$), 7.38–7.40 (m, 4H, Ar), 5.10 (s, 2H, Ar–CH_2–Ar). $^{31}P\{^1H\}$ NMR (161.9 MHz, DMSO-d_6): δ 87.3 (s), $^1J_{PtP}$ = 3896 Hz.

Synthesis of [Au(Cl){η^2-$Ph_2P(–OC_{10}H_6)(\mu$-$CH_2)(C_{10}H_6O–)$-PPh_2-κ*P*,κ*P*}] (9)

A solution of the ligand **1** (0.068 g, 0.102 mmol) in 8 mL of CH_2Cl_2 was added dropwise to a solution of [AuCl(SMe$_2$)] (0.03 g, 0.102 mmol), also in CH_2Cl_2 (6 mL) and the mixture was stirred for 6 h at room temperature. The colourless solution was concentrated to 3 mL and layered with 1 mL of petroleum ether, which on cooling to −25 °C gave **9** as analytically pure, white crystals. Yield: 78% (0.072 g). Mp 170–172 °C. Anal. Calc. for $C_{45}H_{34}ClO_2P_2Au$: C, 59.98; H, 3.80%. Found: C, 59.87; H, 3.76%. ^1H NMR (400 MHz, $CDCl_3$): δ 8.21 (d, 2H, Ar), 8.03 (d, 2H, Ar), 7.68–7.73 (m, 2H, Ar), 7.48–7.58 (m, 20H, $OPPh_2$), 7.43 (t, 2H, Ar), 7.34 (d, 2H, Ar), 6.84 (d, 2H, Ar), 4.79 (s, 2H, Ar–CH_2–Ar). $^{31}P\{^1H\}$ NMR (161.9 MHz, $CDCl_3$): δ 136.1 (br). ESI MS: 865.6 (M^+ − Cl).

Synthesis of [AuCl{$Ph_2P(–OC_{10}H_6)(\mu$-$CH_2)(C_{10}H_6O–)$-PPh_2}AuCl] (10)

A solution of the ligand **1** (0.045 g, 0.067 mmol) in 8 mL of CH_2Cl_2 was added dropwise to a solution of [AuCl(SMe$_2$)] (0.04 g, 0.136 mmol), also in CH_2Cl_2 (6 mL) and stirred for 6 h at room temperature. The colourless solution was concentrated to 3 mL and layered with 1 mL of petroleum ether, which on cooling to −25 °C gave **10** as analytically pure, white crystals. Yield: 86% (0.065 g). Mp 176–178 °C. Anal. Calc. for $C_{45}H_{34}Cl_2O_2P_2Au_2$: C, 47.68; H, 3.02%. Found: C, 47.46; H, 2.98%. ^1H NMR (400 MHz, $CDCl_3$): δ 8.03 (d, 2H, Ar), 7.67–7.73 (m, 2H, Ar), 7.61 (d, 2H, Ar), 7.48–7.51 (m, 2H, Ar), 7.40–7.48 (m, 20H, $OPPh_2$), 7.25–7.35 (m, 2H, Ar), 7.08 (d, 2H, Ar), 4.70 (s, 2H, Ar–CH_2–Ar). $^{31}P\{^1H\}$ NMR (161.9 MHz, $CDCl_3$): δ 111.7 (s). ESI MS: 1097.9 (M^+ − Cl), 865.0 (M^+ − $AuCl_2$).

General procedure for the coupling reactions of aryl halides with boronic acids

In a two-necked round bottom flask under an atmosphere of nitrogen were placed the appropriate amount of Pd(OAc)$_2$ (0.5 or 1 mol%) and 1.2 equivalent of ligand **1**, and 5 mL of methanol was added to it. After stirring for 5 min, aryl halide (0.5 mmol), aryl boronic acid (0.75 mmol) and K_2CO_3 (0.138 g, 1 mmol) were introduced into the reaction flask. The mixture was stirred at room temperature or 60 °C for 1 or 2 h under an atmosphere of nitrogen (the course of reaction was monitored by GC analysis). Then the solvent was removed under reduced pressure. The resultant residual mixture was diluted with H_2O (10 mL) and Et_2O (10 mL), followed by extraction twice (2 × 6 mL) with Et_2O. The combined organic fraction was dried ($MgSO_4$), stripped of the solvent under vacuum and the residue was redissolved in 5 mL of dichloromethane. An aliquot was taken with a syringe and subjected to GC analysis. Yields were calculated *vs.* aryl halides or dodecane as an internal standard.

Hydrogenation reactions (general procedure)

A combination of 5 mg (0.0051 mmol) of $[Rh(COD)\{Ph_2P\text{-}(\text{–}OC_{10}H_6)(\mu\text{-}CH_2)(C_{10}H_6O\text{–})PPh_2\text{-}\kappa P,\kappa P\}][BF_4]$, 5.1 mmol of substrate and 0.035 mL (0.255 mmol) of triethylamine was dissolved in 20 mL of THF and was introduced into a 50 mL glass vessel. The glass vessel containing the reaction mixture was placed in the steel autoclave and the reactor was sealed. The vessel was purged three times with hydrogen and then the autoclave was pressurized with 100 psi of hydrogen. The reaction mixture was stirred at the desired temperature for the required time. The extent of conversion was determined by periodic GC analysis until the desired conversion (partial or complete) was attained.

X-Ray crystallography

A crystal of each of the compounds **2**, **6**, **7**, **9** and **10** suitable for X-ray crystal analysis was mounted in a Cryoloop™ with a drop of Paratone oil and placed in the cold nitrogen stream of the Kryoflex™ attachment of the Bruker APEX CCD diffractometer. A full sphere of data was collected using 606 scans in ω (0.3° per scan) at $\phi = 0$, 120 and 240° using the SMART software package [Bruker-AXS, SMART, Version 5.625, Madison, WI (2000)]. The raw data were reduced to F^2 values using the SAINT+ software [Bruker-AXS, SAINT+, Version 6.35A, Madison, WI (2002)] and a global refinement of unit cell parameters using 6500–8500 reflections chosen from the full data set was performed. Multiple measurements of equivalent reflections provided the basis for an empirical absorption correction as well as a correction for any crystal deterioration during the data collection [SADABS (G. M. Sheldrick, SADABS, Version 2.05. University of Göttingen, Germany (2002)]. The structures were solved by direct methods (for **6** and **7**) or the position of the metal atoms were obtained from a sharpened Patterson function (for **2**, **9** and **10**) and refined by full-matrix least-squares procedures using the SHELXTL program package [Bruker-AXS, SHELXTL, Version 6.10, Madison, WI (2000); G. M. Sheldrick, SHELXS97 and SHELXL97. University of Göttingen, Germany (1997)]. Hydrogen atoms were placed in calculated positions and included as riding contributions with isotropic displacement parameters tied to those of the attached non-hydrogen atoms.

CCDC reference numbers 279236 (**2**), 279236 (**6**), 279236 (**7**), 279236 (**9**) and 279236 (**10**).

For crystallographic data in CIF or other electronic format see DOI: 10.1039/b510589g

Acknowledgements

We are grateful to the Department of Science and Technology (DST), New Delhi for funding through grant SR/S1/IC-05/2003. B. P. thanks CSIR for Research Fellowship (J. R. F. and S. R. F.). We also thank RSIC, Mumbai, Department of Chemistry Instrumentation Facilities, Bombay, for spectral and analytical data and J. T. M. thanks the Louisiana Board of Regents through grant LEQSF(2002-03)-ENH-TR-67 for purchase of the CCD diffractometer and the Chemistry Department of Tulane University for support of the X-ray laboratory.

References

1 (*a*) *Homogeneous Catalysis with Metal Phosphine Complexes*, ed. L. H. Pignolet, Plenum, New York, 1983; (*b*) G. J. H. Buisman, L. A. van der Veen, A. Klootwijk, W. G. J. de Lange, P. C. J. Kamer, P. W. N. M. van Leewen and D. Vogt, *Organometallics*, 1997, **16**, 2929; (*c*) D. Gleich, R. Schmid and W. A. Herrmann, *Organometallics*, 1998, **17**, 2141; (*d*) R. C. Smith and J. D. Protasiewicz, *Organometallics*, 2004, **23**, 4215; (*e*) S. Basra, J. G. de Vries, D. J. Hyett, G. Harrison, K. M. Heslop, A. G. Orpen, P. G. Pringle and K. von der Luehe, *Dalton Trans.*, 2004, 1901; (*f*) J. I. van der Vlugt, R. Sablong, A. M. Mills, H. Kooijman, A. L. Spek, A. Meetsma and D. Vogt, *Dalton Trans.*, 2003, 4690; (*g*) A. Pintado-Alba, H. de la Riva, M. Nieuwhuyzen, D. Bautista, P. R. Raithby, H. A. Sparkes, S. J. Teat, J. M. López-de-Luzuriaga and M. C. Lagunas, *Dalton Trans.*, 2004, 3459.

2 (*a*) R. Guo, A. J. Lough, R. H. Morris and D. Song, *Organometallics*, 2004, **23**, 5524; (*b*) B. Kesanli and W. Lin, *Chem. Commun.*, 2004, 2284; (*c*) M. Hölscher, G. Franciò and W. Leitner, *Organometallics*, 2004, **23**, 5606; (*d*) J. A. Wiles, C. J. A. Daley, R. J. Hamilton, C. G. Leong and S. H. Bergens, *Organometallics*, 2004, **23**, 4564.

3 J. J. Carbó, F. Maseras, C. Bo and P. W. N. M. van Leeuwen, *J. Am. Chem. Soc.*, 2001, **123**, 7630.

4 M. S. Balakrishna, R. Panda and J. T. Mague, *J. Chem. Soc., Dalton Trans.*, 2002, 4617.

5 (*a*) M. S. Balakrishna, K. Ramaswamy and R. M. Abhyankar, *J. Organomet. Chem.*, 1998, **560**, 131; (*b*) M. S. Balakrishna, R. M. Abhyankar and J. T. Mague, *J. Chem. Soc., Dalton Trans.*, 1999, 1407; (*c*) M. S. Balakrishna, R. Panda and J. T. Mague, *Inorg. Chem.*, 2001, **40**, 5620; (*d*) S. Priya, M. S. Balakrishna and J. T. Mague, *Inorg. Chem. Commun.*, 2001, 437; (*e*) M. S. Balakrishna and R. McDonald, *Inorg. Chem. Commun.*, 2002, **5**, 782; (*f*) S. Priya, M. S. Balakrishna, J. T. Mague and S. M. Mobin, *Inorg. Chem.*, 2003, **42**, 1272; (*g*) S. Priya, M. S. Balakrishna, S. M. Mobin and R. McDonald, *J. Organomet. Chem.*, 2003, **688**, 227; (*h*) M. S. Balakrishna, P. P. George and J. T. Mague, *J. Organomet. Chem.*, 2004, **689**, 3388.

6 S. Priya, M. S. Balakrishna and J. T. Mague, *J. Organomet. Chem.*, 2004, **689**, 3335.

7 E. K. van den Beuken, W. G. J. de Lange, P. W. N. M. van Leeuwen, N. Veldman, A. L. Spek and B. L. Feringa, *J. Chem. Soc., Dalton Trans.*, 1996, 3561.

8 (*a*) J. P. Wolfe and S. L. Buchwald, *Angew. Chem., Int. Ed.*, 1999, **38**, 2413; (*b*) J. P. Wolfe, R. A. Singer, B. H. Yang and S. L. Buchwald, *J. Am. Chem. Soc.*, 1999, **121**, 9550.

9 A. F. Littke, C. Dai and G. C. Fu, *J. Am. Chem. Soc.*, 2000, **122**, 4020.

10 T. J. Colacot, H. Qian, R. Cea-Olivares and S. Hernandez-Ortega, *J. Organomet. Chem.*, 2001, **637–639**, 691.

11 R. B. Bedford, S. M. Draper, P. N. Scully and S. L. Welch, *New J. Chem.*, 2000, **24**, 745.

12 R. B. Bedford, S. L. Hazelwood, M. E. Limmert, J. M. Brown, S. Ramdeehul, A. R. Cowley, S. J. Coles and M. B. Hursthouse, *Organometallics*, 2003, **22**, 1364.

13 I. Moldes, E. de la Encarnacion, J. Ros, A. Alvarez-Larena and J. F. Piniella, *J. Organomet. Chem.*, 1998, **566**, 165.

14 (*a*) J. A. Widegren, M. A. Bennett and R. G. Finke, *J. Am. Chem. Soc.*, 2003, **125**, 10301; (*b*) J. A. Widegren and R. G. Finke, *J. Mol. Catal. A: Chem.*, 2003, **198**, 317.

15 D. J. Darensbourg and R. L. Kump, *Inorg. Chem.*, 1978, **17**, 2680.

16 G. Giordano and R. H. Crabtree, *Inorg. Synth.*, 1990, **28**, 88.

17 J. A. McCleverty and G. Wilkinson, *Inorg. Synth.*, 1990, **28**, 84.

18 Y. Tatsuno, T. Yoshida and S. Otsuka, *Inorg. Synth.*, 1990, **28**, 342.

19 H. C. Clark and L. E. Manzer, *J. Organomet. Chem.*, 1973, **59**, 411.

20 M. C. Brandys, M. C. Jennings and R. J. Puddephatt, *J. Chem. Soc., Dalton Trans.*, 2000, 4601.